INDIAN OCEAN HYDROACOUSTIC WAVE PROPAGATION CHARACTERISTICS

Pierre-Franck Piserchia, Pierre-Mathieu Dordain
CEA/DIF – Département Anlayse, Surveillance, Environnement, France

Sponsor
Commissariat à l'Energie Atomique (CEA), France

ABSTRACT

The channeling efficiency of the Deep Sound Channel (often referred as the Sofar channel) allows long range propagation of hydroacoustic waves over a few thousands of kilometers. Strong T-waves, referring to a third arrival on seismic waves, are commonly observed on underwater receivers (hydrophones stations) and on coastal receivers (T-phase stations), when an oceanic earthquake or an underwater explosion occurs, even for small events. Consequently, to insure the verification of the Comprehensive Nuclear-Test-Ban Treaty (CTBT), the hydroacoustic network of the International Monitoring System (IMS) uses five T-phase stations and six hydrophones. At the end of 2001, three hydrophone stations -HA1 at Cape Leeuwin, HA4 at Crozet, and HA8 at Diego Garcia will continuously send their data to the IMS. These data will also be available at National Data Centers. Then, using these data it will be possible 1) to refine the network detection capability 2) to estimate the network localization precision and 3) to estimate the transmission loss of the hydroacoustic propagation and the hydroacoustic-to-seismic conversion at the T-phase stations. To prepare this evaluation, we are studying the underwater propagation in the region of the Indian Ocean and in the South Atlantic Ocean using modeling approaches.

The first part of this paper gives a general view of the variation of the bathymetry, the sound speed propagation and the Sofar channel axis in the Indian Ocean. In particular, it is shown that there is a strong sound speed profile variation, from the North to South Indian Ocean, due to a cold water front coming from the Sub-Antarctic Ocean. In a second part, three areas are defined in the region of the Indian Ocean and in the Antarctic Ocean. In each of them, a typical sound speed profile has been considered to estimate numerically the underwater transmission loss characteristics. The underwater blockage effect due to underwater seamounts are also investigated in this part. In the three regions previously defined, this approach allows us to propose a basic formulation of the transmission loss (TL in dB) :

$$TL(f_s, z_s, r) = A_o(f_s, z_s) + 10 \cdot \log(r) + B(f_s, z_s) + \alpha(f_s) \cdot (r - 1)$$

where f_s, z_s, r are respectively the frequency, the depth, the distance of the underwater source and α is the absorption coefficient. These laws could give a good and simple characterization of the transmission loss and can be used to estimate quickly the source charge weight from an hydroacoustic record of an underwater blast. In this preliminary study, A_o and B are estimated numerically using a parabolic equation technique in the frequency domain. In the discussion, we investigate the number of record points and source localization which are necessary to provide a good estimation of A_o and B .

Objective:

At the end of 2001, three hydrophone stations (Figure 1). -HA1 at Cape Leeuwin, HA4 at Crozet, HA8 at Diego Garcia - will continuously send their data to the IMS. These data will also be available at National Data Centers. Then, using these data it will be possible 1) to refine the network detection capability 2) to estimate the network localization precision and 3) to estimate the transmission loss. The objective of this research is to study the underwater propagation in the region of the Indian Ocean using modeling approaches to prepare an experimental evaluation of the IMS hydroacoustic network in the Indian Ocean. We are in particular investigating the transmission loss and blockage effects due to sea mounts or underwater plateaus.

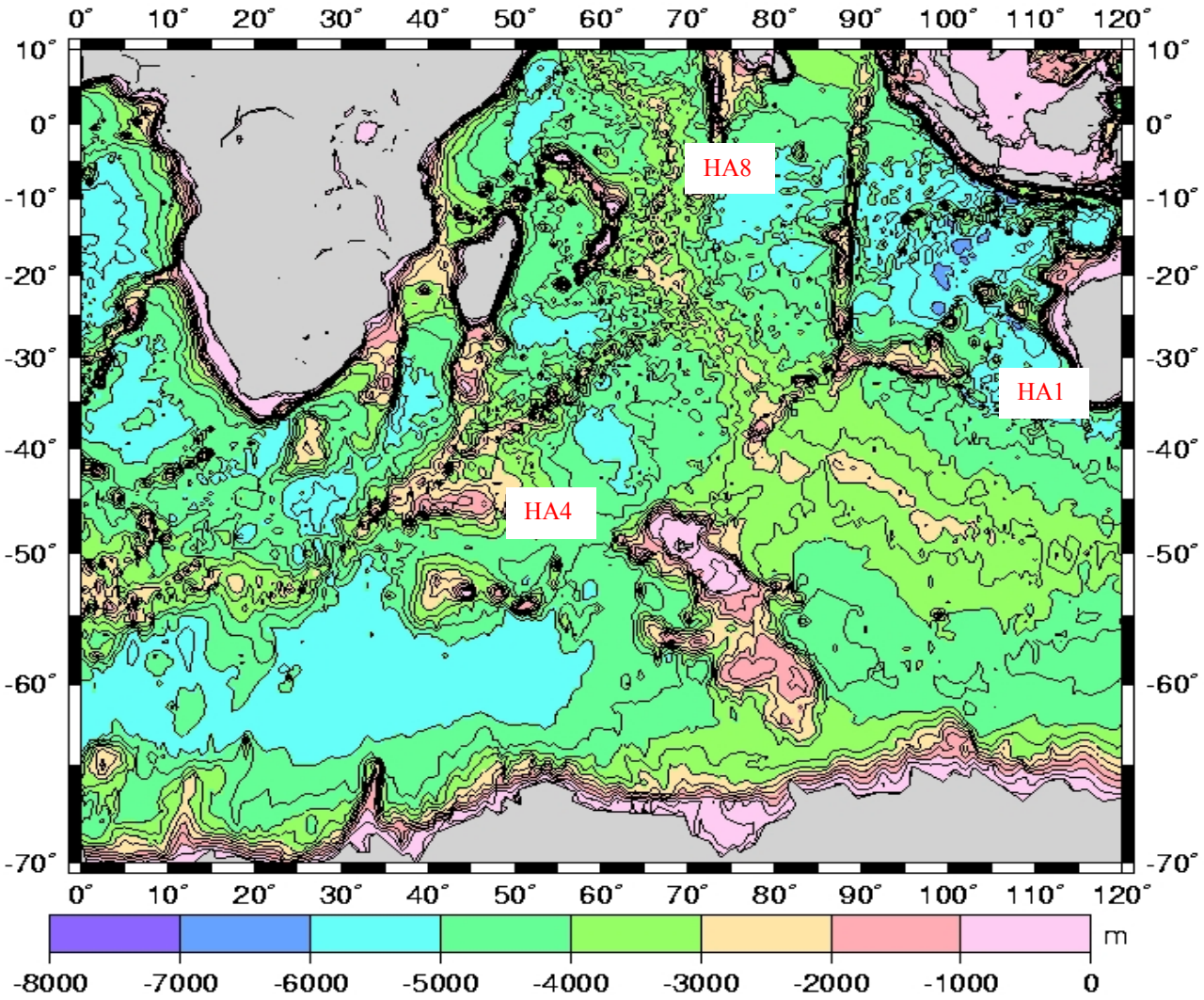

Figure 1 : Indian Ocean map. Three hydrophone stations participate to the International Monitoring System in the Indian Ocean -HA1 at Cape Leeuwin, HA4 at Crozet, HA8 at Diego Garcia.

Research accomplished :

The first part of this paper gives a general view of the variation of the bathymetry, the sound speed propagation and the Sofar channel axis in the Indian Ocean. In the second part, we investigate numerically the underwater transmission loss.

Overview of the Indian Ocean main characteristics

Hydroacoustic wave propagation in an ocean is mainly controlled by the velocity variation with respect to depth and range. It is well known that the velocity increases with temperature, salinity and depth. In the Indian Ocean, bands of equal temperatures run east-west. Water temperature is the highest along the equator, because there Earth is most warmed by solar radiation, and become cooler toward Antarctica (Figure 2). Because the temperature decreases with depth, the velocity decays rapidly with depth down to a minimum at the Sofar channel axis. Below this depth, the velocity increases quite linearly with the hydroacoustic pressure. Due to this variations, bands of equal sound speed run east-west and there is a strong sound speed variation on the Sofar channel axis, from about 1500 m/s in the North to 1455 m/s in South Indian Ocean. In our study, we have considered three different types of sound speed profiles (Figure 2).

Hydroacoustic wave propagation in an ocean is also controlled by the bathymetry variation (Figure 1) along the wave path. The Indian Ocean basin is the shallowest of the two other major basins because it is the youngest. This basin has five important ridges that may block hydroacoustic wave propagation. It has three active mid-ocean ridges : the Southwest Indian Ridge, the Southeast Indian Ridge and the Mid-Indian Ridge where there is the strongest seismic activity and two inactive volcanic ridges : the Chagos-Laccadive Plateau and the Ninetyeast Ridge. The large Kerguelen Plateau has also some regional seismic activity.

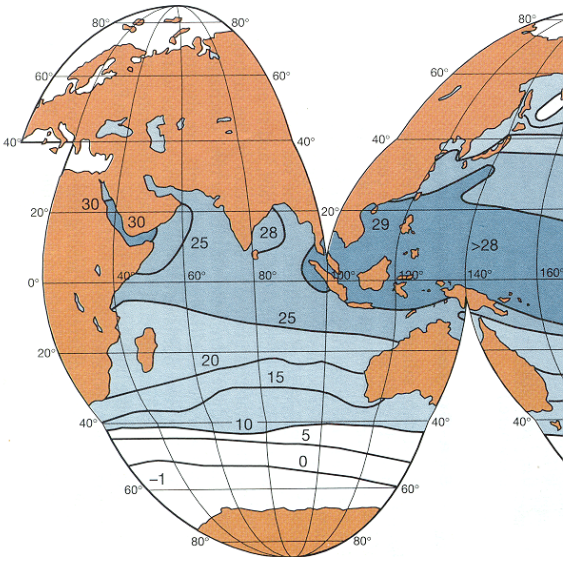

Figure 2 : Ocean surface temperatures (from Gross et al., 1996). In the Indian Ocean, bands of equal temperatures run east-west. Water temperatures are the highest along the equator, because there Earth is most warmed by solar radiation, and become cooler toward Antarctica. Note the presence of a cold water front at the latitude 40°.

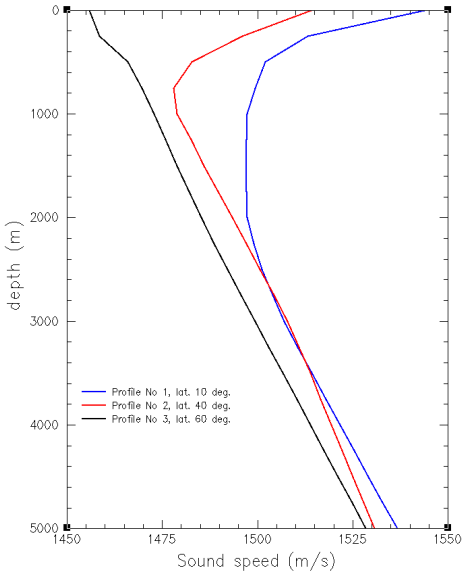

Figure 3 : Ocean Indian sound speed variation. The Sofar channel axis depth decreases from North (blue profile) to South (black profile) to reach the sea surface. Note a strong sound speed variation on the Sofar channel axis, from about 1500 m/s in the North to 1455 m/s in the South.

Transmission loss estimation from modeling

Our strategy

After an underwater explosion occurs, only a portion of energy is trapped in the Sofar channel (Piserchia et al, 1998) allowing propagation of waves over large distances without any reflection losses at sea flour and sea surface. As we will see in this paper, the trapped energy flux depends on the Sofar channel characteristics, the source depth and the source frequency. It is well known, that the transmission loss of this energy is mainly due to the geometrical attenuation, blockage effects and absorption. To investigate the roles played by the source and Sofar characteristics as well as the blockage effects, the basic transmission loss formulation (TL in dB ref. 1 m):

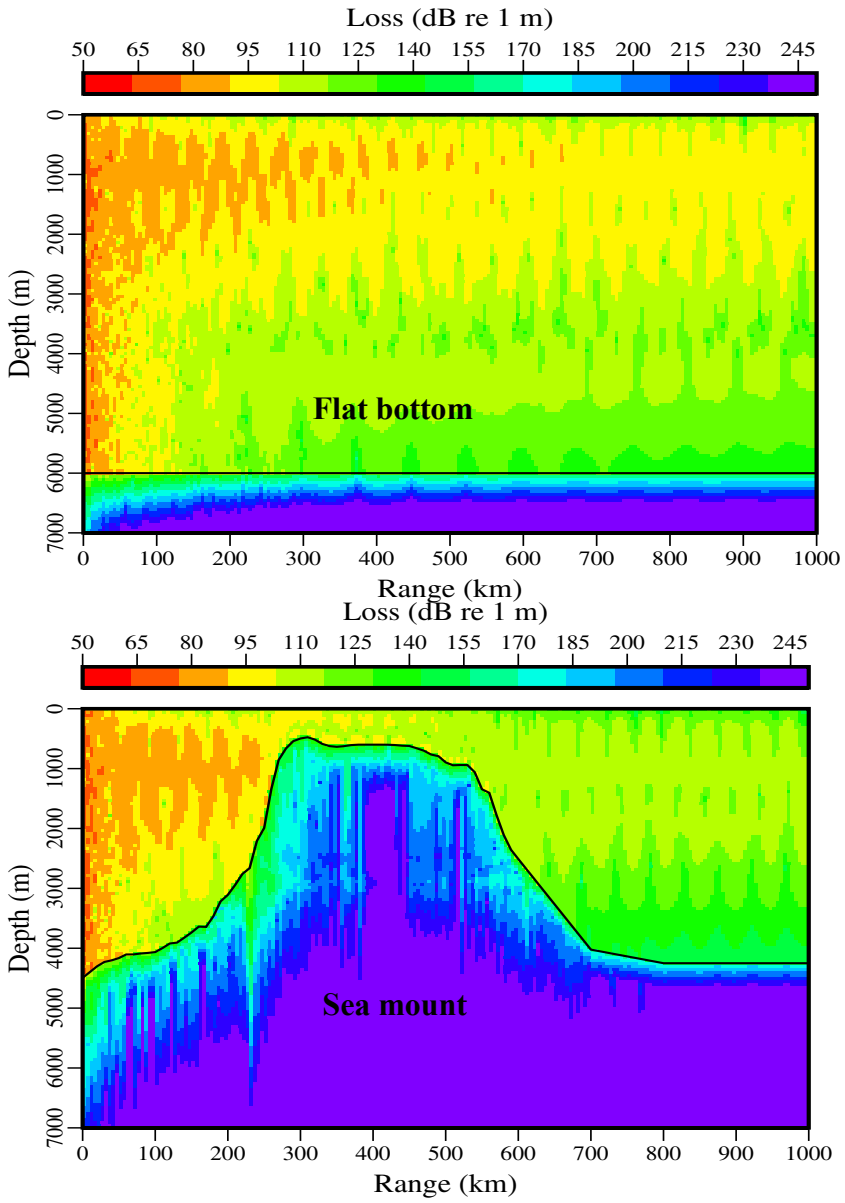

Figure 4 : Two cases of underwater propagation using the profile n°2. A 10 Hz isotropic source is located on the Sofar channel axis at 800 m in a flat bottom ocean in the first case and in front of a sea mount in the second case. These two color images of the transmission loss have been computed by the

code RAMS. In the first case, the transmission loss (in dB ref. 1 m) can be approximated by TL = 35 + 10 log(r) whereas in the second case we obtain TL = 35 + 10 log(r) + 15.

$$TL(f_s, z_s, r) = A_o(f_s, z_s) + 10 \cdot \log(r) + B(f_s, z_s) \quad (1)$$

as been considered. The source may vary with depth and frequency and the receiver is always considered to be on the Sofar channel axis. f_s, z_s, r are respectively the frequency (in Hertz), the depth (in meter), the distance (in meter) of the underwater source.

A0 represents the trapped energy at 1m in Sofar channel. *A0* decreases when the trapped energy increases. The second term *10 log(r)* represents the attenuation due to the cylindrical spreading. The second parameter *B* represents additional attenuations due to blockage effects. In this preliminary study, *A0* and *B* were numerically estimated in the three previous regions we defined. The code RAMS is used to solve the Helmoltz equation using the parabolic equation approximation in the frequency domain (Collins, 1993). In a first step, we computed the transmission loss in the three regions. Then, in a second step, *A0* and *B* are computed minimizing the difference between the numerical estimation and our formulation (1).

Numerical results

Tables 1 and 2 represent the numerical estimation of *A0* in two regions located in the north of the cold water front. In these two regions, *A0* is evaluated with a standard deviation error lower than 5 dB. In both cases, when the source is on the Sofar channel axis respectively at 1500 m (profile n°1) and 800 m (profile n°2), *A0* reaches a minimum equal to 38 dB and 35 dB. We re-find the well known property that the transmission loss is minimum when the source is on the Sofar Channel axis. When the source goes closer to the Sofar channel limits near the surface (at 100 m) or the sea bottom (at 5000 m), *A0* and therefore the transmission loss can increase up to 13 dB at 10 Hz. This additional loss is all the more important that the frequency is low. In the frequency range 5 to 15 Hz, this additional loss is always higher than 10 dB. An under evaluation of 10 dB of the level would lead to an under charge weight estimation of a factor 10. Table 3 gives the results we obtained in the Antarctic Ocean. In this region, because the minimum sound speed zone is at the sea surface, there are reflections losses. *A0* must be interpreted cautiously because our modeling do not take into account of these losses.

Variation A_0 of with the source location and frequency

Profile n°1	Zs=100 m	Zs=500 m	Zs=800 m	Zs=1500 m	Zs=5000 m
5 Hz	53 dB	42 dB	41 dB	38 dB	57 dB
10 Hz	51 dB	42 dB	41 dB	38 dB	49 dB
15 Hz	50 dB	42 dB	41 dB	38 dB	48 dB

Tab. 1 : A_0 estimation in the region n°1 at the North of the Indian Ocean. The minimum sound speed zone is close to 1500 m.

Profile n°2	Zs=100 m	Zs=500 m	Zs=800 m	Zs=1500 m	Zs=5000 m
5 Hz	52 dB	39 dB	35 dB	39 dB	57 dB
10 Hz	48 dB	39 dB	35 dB	40 dB	49 dB
15 Hz	46 dB	39 dB	36 dB	41 dB	48 dB

Tab. 2 : A_0 estimation in the region n°2 at the South of the Indian Ocean. The minimum sound speed zone is close to 800 m.

Profile n°3	Zs=100 m	Zs=500 m	Zs=800 m	Zs=1500 m	Zs=5000 m
5 Hz	45 dB	35 dB	35 dB	38 dB	53 dB
10 Hz	38 dB	33 dB	38 dB	44 dB	48 dB
15 Hz	35 dB	37 dB	40 dB	39 dB	47 dB

Tab. 3 : A_0 estimation in the region n°3 in the Antarctic Ocean.

These results demonstrate that it is important to know the variation of the transmission loss with the source depth variation in each regions of the Indian Ocean. They have been obtain considering a flat bottom ocean. As it has been said in a previous part the Indian Ocean basin has five important ridges that could generate hydroacoustic wave blockage effects. As an illustration of these effects, Figure 4, gives two cases of underwater propagation using the profile n°2. A 10 Hz isotropic source is located on the Sofar channel axis in a flat ocean bottom in the first case and in a front of a sea mount in the second case. In the first example, the transmission loss can be approximated by TL = 35 + 10 log(r) whereas in the second example we obtain TL = 35 + 10 log(r) + 15. The additional increased of 15 dB is due the blockage effects of the sea mount. Figure 5 illustrates an other example of underwater blockage due to a sea mount. The transmission loss after the sea mount is compared with the transmission loss in a flat ocean sea bottom. In this example, it is shown that the addition loss increases with the frequency decayed from 5 dB at 5 Hz to 15 dB at 15 Hz. An under estimation of 15 dB of the source level could lead to an under charge weight evaluation of a factor 30.

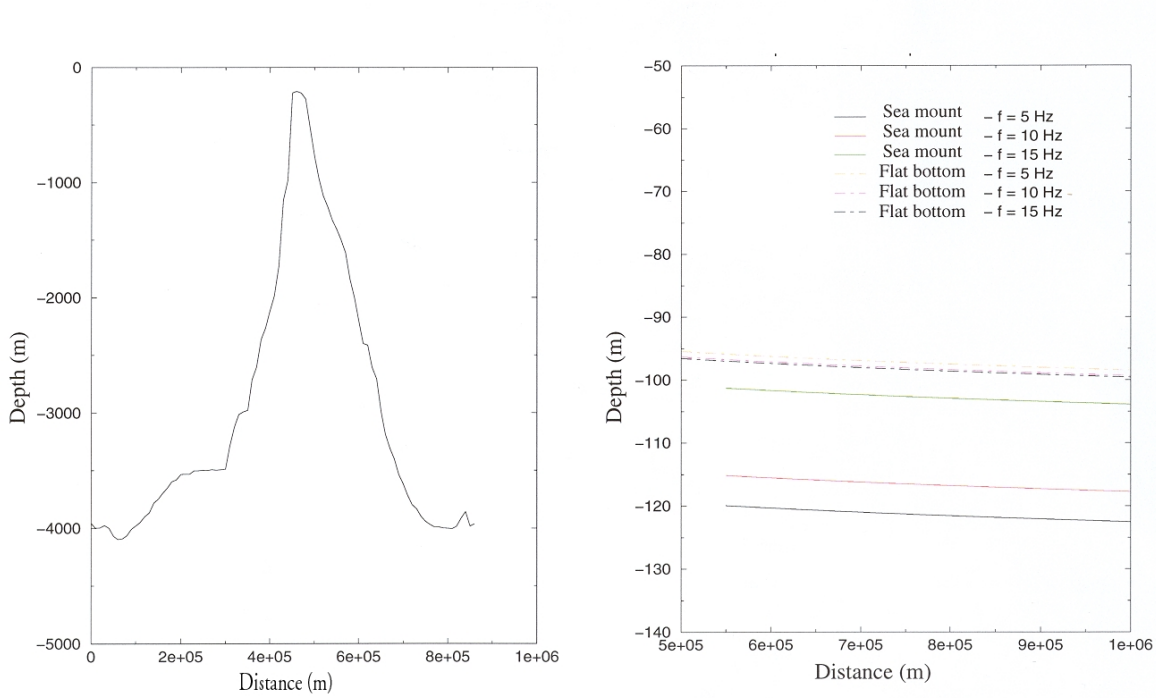

Figure 5 : Blockage effects due to an underwater sea mount. The source is located in front of the sea mount on the Sofar channel axis. The figure on the right represents the transmission loss variation with range and frequency behind the sea mount.

Discussion

We investigated numerically the number of record points and source localization which are necessary to provide a good estimation of *A0* and *B*. In this paper, the transmission loss was computed every 500 m by the code RAMS. Then in a second step, *A0* was evaluated to minimize the difference between the numerical estimation and our formulation (1). In a numerical parameterized study, we found that a distance between points smaller than 400 km and more than three points of records are needed to insure an acceptable error lower than 5 dB on the *A0* calculation.

Conclusions and Recommendations :

As it has been recommended at the *Tahiti Hydroacoustic Workshop* (organized by CTBTO and CEA/DASE in September 1999), we believe that it is necessary to calibrate the hydroacoustic network of the International Monitoring System in the Indian Ocean. This study demonstrates that the transmission loss may vary with the source depth and from one region of the Indian Ocean to an other. This is the reason why we believe that the transmission loss should be studied carefully in particular to validate model calculations used to estimated source levels. During the definition of the calibration experiment, we recommend to also investigate source geometry to analyze transmission loss phenomena and blockage effects.

Key Words : T-phase, hydroacoustic, Indian Ocean propagation, transmission loss

References :

Collins, M.D., A higher-order energy-conserving parabolic equation for range-dependent ocean depth, sound speed, and density, J. Acoust. Soc. Am., 101, 1068-1075, 1993.

CTBTO/PTS, CEA/DASE, Informal workshop on “hydroacoustics”, French Polynesia Tahiti, Conference proceeding, September 1999.

Gross, M. G., Gross, E.. *Oceaography*, seventh edition, NJ : Prentice Hall, 1996.

Levitus, S., Boyer, T. Antonov, J., Burgett, R., and Conkright, M., World Ocean Atlas 1994, NOAA/NESDIS, Silver Springs, Maryland, 1994.

Piserchia, P.-F, Rodrigues, D., Virieux J., Gaffet S., Detection of underwater explosions from very long range records, Oceans’98 , Nice, Conference proceeding, vol. 2, 698-702, 1998.